

Initial Study of the Distributed Cavity Phase Shift for the New Microwave Cavities of Cs Fountains at NIST

Gregory W. Hoth, Bijunath Patla, Neil Ashby, Vladislav Gerginov

NIST Time and Frequency Division

Boulder, CO USA

gregory.hoth@nist.gov

Summary—The microwave cavities of NIST-F1, the cesium fountain primary frequency standard at the National Institute of Standards and Technology (NIST), have been replaced with a new design. The distributed cavity phase (DCP) bias of the new cavity must be investigated. Here, we describe an initial study of the DCP bias using the techniques developed by Li and Gibble [Li and Gibble, *Metrologia* 41 (2004); Li and Gibble, *Metrologia* 47 (2010)]. We solve for the field distribution in the Ramsey cavity using a relatively simple 3D finite element model. Density matrix simulations using this field model suggest that the DCP errors of the new cavity design are manageably small.

Keywords—Cesium fountain clock; distributed cavity phase shift; finite element modeling frequency bias

I. INTRODUCTION

NIST-F1 is a primary cesium fountain frequency standard developed by the National Institute of Standards and Technology (NIST) [1]. It was first evaluated as a frequency standard nearly twenty years ago, but recent changes to the apparatus have led us to begin a re-evaluation of NIST-F1's accuracy. Several years ago, NIST-F1's state selection and Ramsey cavities were replaced with a new design. These cavities have a radius $R = 30$ mm and two diametrically opposed feeds centered on the cavity sidewalls. They are made from aluminum (Al 6061 T6, conductivity $\sigma = 2.5 \times 10^7$ S/m) rather than copper ($\sigma = 5.8 \times 10^7$ S/m). Also, the apertures in the endcaps, which allow cold atoms to pass through the cavity, are asymmetric. For the Ramsey cavity, the aperture in the upper endcap has a radius $r_{a,1} = 7.2$ mm, while the aperture in the lower endcap has a radius $r_{a,2} = 5.5$ mm. The effect of this new cavity design on the fountain's performance must be evaluated.

The distributed cavity phase (DCP) bias is a first-order Doppler shift due to cold atoms moving through phase gradients in the Ramsey cavity. The spatial phase variations are caused by the finite conductivity of the cavity walls and endcaps [2-4]. The DCP bias can be calculated with the methods developed by Li and Gibble [3-8]. In their approach, the deviation of the cavity field from a perfect standing wave is obtained from a finite element model. Then, the field is used to solve the density matrix equations for a distribution of atomic trajectories. For fountain cavities with cylindrical symmetry, the cavity field can be obtained from a set of 2D finite element calculations [3,4], but the method has also been implemented in 3D [8]. Previous work at NIST towards understanding the DCP bias and microwave power dependence in Cs fountains at NIST

relied on analytical methods rather than the numerical methods developed by Li and Gibble and discussed here [9].

The field modeling approach of Li and Gibble can be used to accurately quantify the DCP bias [5], but it requires significant development to implement. For an initial study of the DCP errors of NIST-F1's new cavity, we have investigated a simple 3D finite element model [10-12] that solves for the whole cavity field rather than isolating the deviations from a standing wave. Although our approach is less accurate, it is straightforward to implement, and we obtain field models that appear suitable for an initial estimate of the DCP bias. We find that the DCP errors are manageably small despite the cavity's unusual features.

II. REVIEW OF DCP THEORY

Li and Gibble [3,4] have developed a complete theory of the DCP bias for cold atom fountains. Here, we summarize some of their results which are applicable to our study. For a cylindrical fountain cavity, it is useful to treat the cavity field as a Fourier series in $\cos(m\phi)$ where m is an integer and ϕ is the angular variable in cylindrical coordinates. Typically, it is only necessary to consider terms $m = (0, 1, 2)$ because further terms are small due to the convergence of the Fourier series and suppressed by averaging over the atomic distribution [3, 4]. After we solve for the field in 3D, we convert the field into a Fourier series in $\cos(m\phi)$ for further analysis.

The bias caused by the cavity phase gradients can be quantified by computing the asymmetry in the transition probability between the two sides of the Ramsey fringe as a function of microwave amplitude, A . The asymmetry can be expressed as $\Delta P(A) = \frac{1}{2} \left(P\left(A, \frac{\Delta\nu}{4}\right) - P\left(A, -\frac{\Delta\nu}{4}\right) \right)$ where $\Delta\nu$ is the fringe spacing and $P(A, \nu)$ is the average transition probability for microwave amplitude A and frequency ν [5]. The frequency shift is proportional to ΔP divided by the contrast of the Ramsey fringes.

The general theory of the DCP bias allows us to predict some consequences of the asymmetric Al cavity. For a particular trajectory through the fountain, ΔP is proportional to the skin depth, $\delta = \sqrt{2/\mu_0\omega\sigma}$ (ω is the angular frequency and μ_0 is the vacuum permeability constant) [4]. Therefore, one expects the DCP effects to be a factor of $\sqrt{\sigma_{Cu}/\sigma_{Al}} \approx 1.5$ larger for an aluminum cavity compared to a copper cavity with the same geometry. From an analysis of the sensitivity function and the

cavity phase variations, one can see that the vertical asymmetry will likely increase the DCP errors near normal power [4].

III. RESULTS

The simplicity of our finite element method raises concerns about the accuracy of the cavity field model, particularly near the edge of the apertures on the cavity endcaps [3,4]. To investigate the quality of the field models obtained with this approach, we have performed several checks. First, we simulate a closed cavity and obtain good agreement with the analytical solution [3]. The results are shown in Fig. 1. Second, we studied models of cavities with endcap apertures for a range of finite element meshes. We model the edge of the aperture with a finite radius of curvature, r_c [4]. Figure 2 illustrates the results of a mesh refinement study for a model of the asymmetric Al cavity where the edge has $r_c = 50 \mu\text{m}$. The solution is well behaved, although some variation can still be seen near the aperture edge with the highest quality mesh. The convergence improves near the edge if the radius of curvature is increased. As a further simplification, we omit atoms that come within 0.1 mm of the aperture edge in our density matrix calculations. This neglects the rapid field variation very close to the aperture's edge. However, these field variations are not expected to cause DCP biases for normal power operation [4]. Finally, we have applied our method to several of the case studies of DCP errors reported in [4] for a copper cavity with $R = 26 \text{ mm}$ and endcap aperture radius $r_a = 5 \text{ mm}$. Our method produces ΔP vs. microwave amplitude curves that are in qualitatively good agreement with the curves reported in [4]. Quantitatively, our simulations reproduce the extrema in the variations of ΔP with microwave amplitude with errors less than 50% up to $9\pi/2$ pulses.

Encouraged by these initial checks, we have studied three cavity models to explore the consequences of the asymmetry and the reduced conductivity. Alongside the asymmetric Al cavity, we consider a copper cavity and an aluminum cavity with symmetric endcaps and $r_a = 5.5 \text{ mm}$. For all three cavities, $R = 30 \text{ mm}$. In each case, the cavity height is tuned to bring the TE_{011} resonance to within 100 kHz of 9.1926 GHz. The cavities are fed with two diametrically opposed feeds centered on the cavity sidewall. The feed radius is 2.4 mm. The models also include a cut-off tube above and below the cavity with the same diameter as the endcap aperture.

To illustrate the DCP bias for these cavities, we solve the density matrix equations for a distribution of trajectories corresponding to a cloud with a Gaussian density profile with initial size $\sigma_0 = 2 \text{ mm}$ and temperature $T = 1 \mu\text{K}$. The cloud is launched vertically, and either centered ($m = 0$) or offset by 2 mm along the feed axis ($m = 2$).

The calculated ΔP vs microwave amplitude curves for $m = 0$ for these three cavities are shown in Fig. 3. As expected, we find that the asymmetry increases ΔP near normal power ($A \approx 1$). For the asymmetric Al cavity, the estimated frequency shift for our test cloud is 0.13×10^{-16} , which is negligible for an accuracy goal in the low 10^{-16} s.

The calculated ΔP vs microwave amplitude curves for $m = 2$ are shown in Fig. 4. For the asymmetric Al cavity, the frequency shift at normal power for the test cloud corresponds

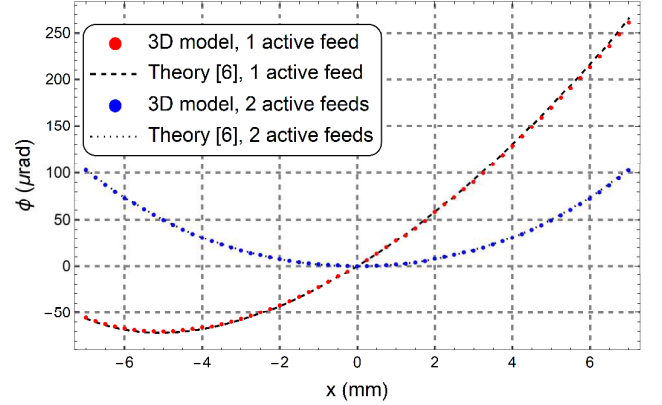


Fig. 1. Phase gradients in H_z along the feed axis predicted by a finite element model compared to the analytic solution [3] for a closed cylindrical cavity with radius $R = 30 \text{ mm}$ and height $h \approx 21.8 \text{ mm}$. The feed radius was 1 mm.

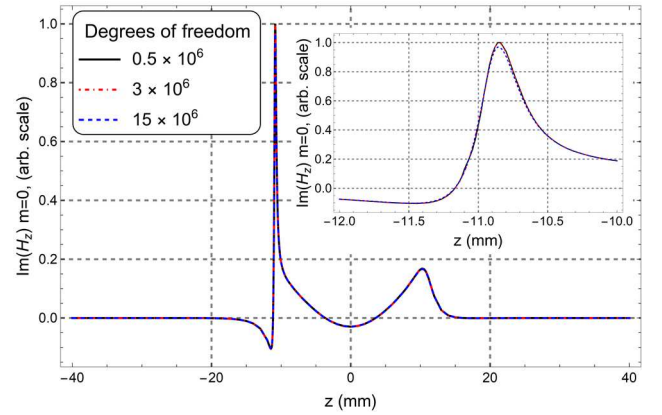


Fig. 2. A mesh refinement study for a finite element model of the asymmetric Al cavity with radius of curvature $r_c = 50 \mu\text{m}$ for the edge of the endcap apertures. We choose a phase convention where H_z is nearly real so that the spatial phase variations are described by $\text{Im}(H_z)$ [3]. We plot the $m = 0$ component of $\text{Im}(H_z)$ along the cavity axis with an offset $r = 5.3 \text{ mm}$ from the cavity center. The apertures ($z \approx \pm 10.9 \text{ mm}$) cause rapid field variations. Outside the cavity, the microwave field amplitude falls off due to the cut-off tubes. The solution appears well converged, although some variation can be seen very close to the lower aperture as shown in the inset. The convergence can be improved by increasing the radius of curvature.

to 3×10^{-16} , which is relatively large and worrisome. For comparison, the $m = 2$ bias has been calculated to be smaller than 0.5×10^{-16} for a 2 mm cloud offset for several fountains with two opposed feeds centered on the cavity sidewall [5, 6]. More recent cavity designs can significantly reduce the $m = 2$ bias so that it becomes negligible [4, 13, 14].

It is interesting to consider why the asymmetric Al cavity has a comparatively large sensitivity to the $m = 2$ bias. As a reference point, case III of [4] considers a similar cloud for a fountain with a copper cavity with $R = 26 \text{ mm}$, $r_a = 5 \text{ mm}$ and finds $\Delta P \approx 2 \text{ ppm}$ (parts per million) near normal power. For the asymmetric Al cavity, we estimate $\Delta P \approx 5 \text{ ppm}$ for our test distribution. Compared to case III of [4], the $m = 2$ bias is increased for the asymmetric Al cavity by the lower

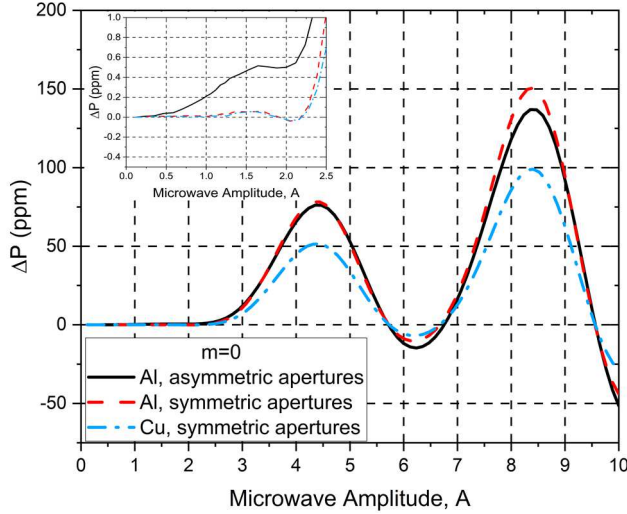


Fig. 3. DCP errors for $m = 0$ as a function of microwave amplitude for three cavity models. The amplitude is normalized so that $A = 1$ corresponds to normal operating power for each case (first maximum in the average transition probability on resonance). The inset shows a zoom for amplitudes close to normal power where the DCP errors are small. At normal power, we estimate $\Delta P \approx 0.2$ ppm or a frequency shift of 1.3×10^{-17} for the asymmetric Al cavity with the test atomic distribution (initial size $\sigma_0 = 2$ mm and temperature $T = 1$ μ K, centered and launched vertically).

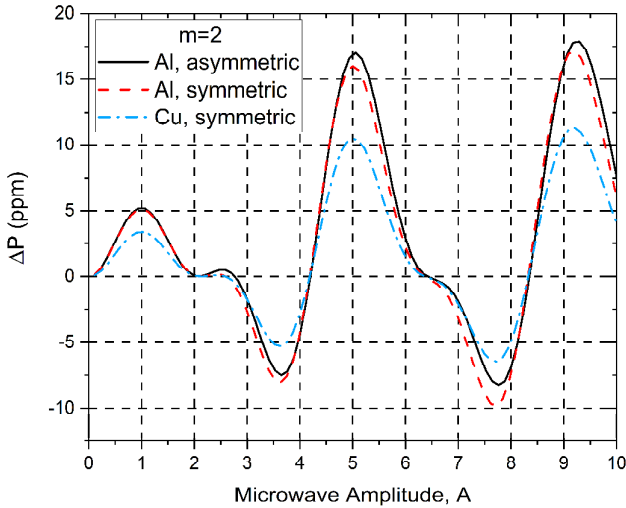


Fig. 4. DCP errors for $m = 2$ as a function of microwave amplitude for three cavity models. The amplitude is normalized so that $A = 1$ corresponds to normal operating power for each case (first maximum in the average transition probability on resonance). At normal power, we estimate $\Delta P \approx 5$ ppm, corresponding to a frequency shift of 3×10^{-16} for the asymmetric Al cavity with the test atomic distribution (initial size $\sigma_0 = 2$ mm and temperature $T = 1$ μ K, launched vertically, offset by 2 mm from the cavity center along the feed axis).

conductivity, the larger cavity radius, and the larger apertures [3].

Another important detail to consider for the $m = 2$ bias is the effect of the TM_{111} mode filters included in many fountain cavities. The mode filter is a groove formed by the cavity walls and the outer edge of the endcaps which acts to shift the TM_{111} resonance away from the TE_{011} resonance [15,16]. Depending

on the dimensions chosen for the groove, the TM_{111} mode filters can have a large effect on the $m = 1$ and $m = 2$ DCP modes [4]. The asymmetric Al cavity of NIST-F1 includes a groove with width 0.13 mm and height 4.8 mm on the upper endcap. For this study, the groove is omitted from our models. Our initial investigations indicate that this mode filter has a small effect on the $m = 2$ bias of the asymmetric Al cavity.

IV. CONCLUSIONS

We have used a relatively simple 3D finite element model for an initial study of the DCP errors in the asymmetric Al cavity currently installed in NIST F1. Our results indicate that although the asymmetry increases the $m = 0$ DCP bias, this bias is likely to be negligible. For the $m = 2$ bias, we estimated a frequency shift of 3×10^{-16} for a molasses-like cloud with a 2 mm offset from the fountain axis. This suggests that the asymmetric Al cavity has a relatively large sensitivity to the $m = 2$ DCP error. This is cause for concern, but an accuracy in the low 10^{-16} s should be achievable once a full evaluation of the DCP bias of NIST F1 is completed. Further investigation of the accuracy of our field model is also needed. It is not clear whether the simple finite element method used in this study could be sufficiently accurate for a full evaluation of the DCP biases for NIST-F1, but the relative simplicity of the method suggests it is a useful tool nonetheless.

This work is a contribution of NIST, a U.S. government agency, and it is not subject to copyright.

REFERENCES

- [1] S. R. Jefferts, J. Shirley, T. E. Parker, D. M. Meekhof, C. Nelson, F. Levi, G. Costanzo, A. De Marchi, R. Drullinger, L. Hollberg, W. D. Lee, and F. L. Walls, "The accuracy evaluation of NIST-F1," *Metrologia*, vol. 39 pp. 321-336 Aug. 2002; T. P. Heavner, S. R. Jefferts, E. A. Donley, J. H. Shirley, and T. E. Parker, "NIST-F1: recent improvements and accuracy evaluations," *Metrologia* vol. 42 p. 411-422 Sept. 2005.
- [2] G. Vecchi and A. De Marchi, "Spatial phase variations in a TE011 microwave cavity for use in a cesium fountain primary frequency standard," *IEEE Trans. Instr. Meas.* vol. 42 pp. 434-438 Apr. 1993
- [3] R. Li and K. Gibble, "Phase variations in microwave cavities for atomic clocks," *Metrologia* vol. 41 pp. 376-386 Oct. 2004.
- [4] R. Li and K. Gibble, "Evaluating and minimizing distributed cavity phase errors in atomic clocks," *Metrologia*, vol. 47 pp. 534-551 Aug. 2010. Li and Gibble 2010
- [5] J. Guéna, R. Li, K. Gibble, S. Bize, and A. Clairon, "Evaluation of Doppler Shifts to Improve the Accuracy of Primary Atomic Fountain Clocks" *Phys. Rev. Lett.* vol. 106 pp. 130801 Apr. 2011.
- [6] S. Weyers, V. Gerginov, N. Nemitz, R. Li, and K. Gibble "Distributed cavity phase frequency shifts of the caesium fountain PTB-CSF2," *Metrologia* vol. 49 pp. 82-87 Nov. 2011.
- [7] R. Li, K. Gibble, and K. Szymaniec, "Improved accuracy of the NPL-CsF2 primary frequency standard: evaluation of distributed cavity phase and microwave lensing frequency shifts," *Metrologia*, vol. 48 pp. 283-289 Aug. 2011.
- [8] Ph. Laurent, F. X. Esnault, K. Gibble, P. Peterman, T. Lévêque, Ch. Delaroche, O. Grosjean, I. Moric, M. Abgrall, D. Massonnet, and Ch. Salomon, "Qualification and frequency accuracy of the space-based primary frequency standard PHARAO," *Metrologia*, vol. 57 pp. 055005 Sept. 2020.
- [9] S. R. Jefferts, J. H. Shirley, N. Ashby, E. A. Burt, and G. J. Dick, "Power dependence of distributed cavity phase-induced frequency biases in atomic fountain frequency standards," *IEEE Trans. Ultrason., Ferroelectr., Freq. Control*, vol. 52, pp. 2314-2321 Dec 2005.

- [10] S. Yanagimachi, Y. Fukuyama, T. Ikegami, and T. Kurosu, "Numerical simulation of distributed cavity phase shift in atomic fountain frequency standard," *Jpn. J. Appl. Phys.* vol. 44 pp. 1468-1475 Mar. 2005.
- [11] L. Devenoges, L.-G. Bernier, J. Morel, G. Di Domenico, A. Jallageas, M. Petersen, and P. Thomann, "Design and Realization of a Low Phase Gradient Microwave Cavity for a Continuous Atomic Fountain Clock," *2013 Joint European Frequency and Time Forum & International Frequency Control Symposium (EFTF/IFC)*, pp. 235-238 2013.
- [12] L. Marmet, P. Dubé, N. Shtin, and R. J. López, "Distributed cavity phase calculation for a rectangular Ramsey cavity in NRC-FCs1," *2013 Joint European Frequency and Time Forum & International Frequency Control Symposium (EFTF/IFC)*, pp. 764-767 2013.
- [13] K. Gibble, S. N. Lea and K. Szymaniec, "A microwave cavity designed to minimize distributed cavity phase errors in a primary cesium frequency standard," *2012 Conference on Precision electromagnetic Measurements*, pp. 700-701 2012.
- [14] S. Beattie, B. Jian, J. Alcock, M. Gertsvolt, R. Hendricks, K. Szymaniec, and K. Gibble, "First accuracy evaluation of the NRC-FCs2 primary frequency standard," *Metrologia*, vol. 57 pp. 035010 Apr. 2020
- [15] E. A. Burt, W. Klipstein, and S. R. Jefferts, "The cesium physics package design for the PARCS experiment," *Proceedings of the 2004 IEEE International Frequency Control Symposium and Exposition*, pp. 71-79 2004.
- [16] R. Schröder, U. Hübner and D. Griebisch, "Design and realization of the microwave cavity in the PTB caesium atomic fountain clock CSF1," *IEEE Trans. Ultrason. Ferroelectr. Freq. Control*, vol. 49 pp. 383-392, March 2002